

A New Process to Develop (100) Texture in Silicon Steel Sheets

T. Tomida

A process for developing (100) texture in silicon steel sheets by manganese removal and decarburization is described. The process consists of annealing in vacuum and subsequent decarburization of conventionally hot- and cold-rolled steel sheets that contain silicon, manganese, and carbon. During the vacuum annealing at α/γ duplex or γ-phase temperatures around 1000 °C, manganese removal occurs and a thin layer near the sheet surface transforms to α. The (100) texture markedly develops in the surface layer. Various types of (100) texture—for example, (100)[021], (100)[001], and (100)[011]—appear at this stage of annealing, depending on processing conditions. During the subsequent decarburization, the grains at the surface layer grow inward as columnar grains retaining the (100) texture. The decarburized steels with a grain size of a few hundred micrometers exhibit excellent soft-magnetic properties.

Keywords

annealing, decarburization, phase transformation, removal of manganese, silicon steel, texture

1. Introduction

A GROWING DEMAND for energy-efficient motors and transformers has created the need for low-loss, high-permeability silicon steel sheets. However, current nonoriented silicon steel sheets, which are essentially isotropic with magnetic properties dependent mainly on chemistry (purity and silicon content) and grain size, are far from the magnetically ideal state. Moreover, grain-oriented silicon steels with (110)[001] possess only one easy magnetizing direction in the sheet plane along the rolling direction. Significant improvements could be realized by developing an ideal texture for which the (100) plane is parallel to the sheet surface. This texture maximizes the number of easy magnetizing directions in the sheet plane. Nevertheless, no commercial steel approaches this (100) texture. This paper describes a process for developing the (100) texture in silicon steel sheets (Ref 1) and shows how this process improves magnetic properties.

The process described here consists of manganese removal and decarburization (MRD process), which has been developed for 2% Si steel sheets (Ref 1). This development is based on the observation that slow transformation and recrystallization near the sheet surface are strongly influenced by the interfacial energy between steel and atmosphere—that is, surface energy (Ref 2-4). The effect of surface energy on recrystallization in high-purity silicon steel sheets has been investigated by many to develop the (100) texture (Ref 2, 3, 5), and it is well known that a secondary recrystallization with the (100) preferred orientation takes place due to the anisotropy of surface energy in some atmospheres, such as a vacuum. However, this method limits thickness of the sheet to values far below that of normal-gage silicon steel sheets (e.g., 0.3 to 0.6 mm). Driving force by surface energy for such recrystallization decreases with increasing sheet thickness (Ref 6). Then it encounters a practical limit of sheet thickness (0.1 to 0.2 mm) (Ref 7). The MRD process is a route to overcome this difficulty.

This process is a two-stage annealing of silicon steel sheets that contain manganese and carbon (Ref 1). During the first vacuum annealing stage, manganese removal occurs and induces a slow transformation from austenite (γ) to α-ferrite (α) near the sheet surface to form a thin, distinct α layer. A pronounced (100) texture is formed in the thin layer; selective driving force for this texture development is believed to be surface energy. In the second stage, decarburization promotes an inward growth of the α grains near the surface and provides the entire sheet with the same texture. Apart from resolving the sheet thickness limitation, a suitably fine grain structure to minimize core loss can also be obtained. In the following sections, details of the MRD process, microstructure and texture evolution during the process, and improved magnetic properties are

T. Tomida, Corporate Research & Development Laboratories, Sumitomo Metal Industries, Ltd., 1-8 Fuso-cho, Amagasaki 660, Japan.

Table 1 Chemical compositions of starting steels

Steel	Composition (a), wt% C	Mn	Si	Al
A	0.096	1.82	2.77	0.002
B	0.097	2.53	2.81	0.002
C	0.050	1.02	2.81	0.002
D	0.096	1.82	2.77	0.002
E	0.051	1.11	3 03	0.001
F	0.050	1.00	2.59	0 001
G	0.050	1.03	2.07	0.001

(a) Determined by the inductively coupled plasma technique.

described using recent results primarily for 3% Si steels. Some of the metallurgical factors involved also are discussed.

2. Procedures

Examples of chemical compositions of starting steels for the MRD process are listed in Table 1. Typical starting steels contain 2 to 3% Si, 1 to 2.5% Mn, and 0.05 to 0.1% C. The steel sheets of this composition (0.3 to 0.5 mm thick) are prepared by conventional casting and rolling processes and are subjected to the final two-stage annealing. The first stage is annealing in a vacuum at temperatures around 1000 °C (for removal of manganese); the second stage is decarburizing annealing in, for instance, a wet hydrogen gas atmosphere in the same temperature range. The chemical composition is controlled so that the steel is of α/γ duplex phase of γ phase at the annealing temperature.

For the experiments described here, vacuum-melted steels of the compositions listed in Table 1 were made at a research laboratory. Resulting ingots from steels A to D were hot rolled to 5.0 mm thick plates with a soaking temperature of 1150 °C, machined to remove oxidized surface layers to 3.0 mm (A and B) and 1.5 mm (C and D) thick plates, and then cold rolled to the final gage of 0.35 mm. The ingots from steels E to G were hot rolled to 4.0 mm thick plates with a soaking temperature of 1200 °C, pickled, and cold rolled to the same final gage.

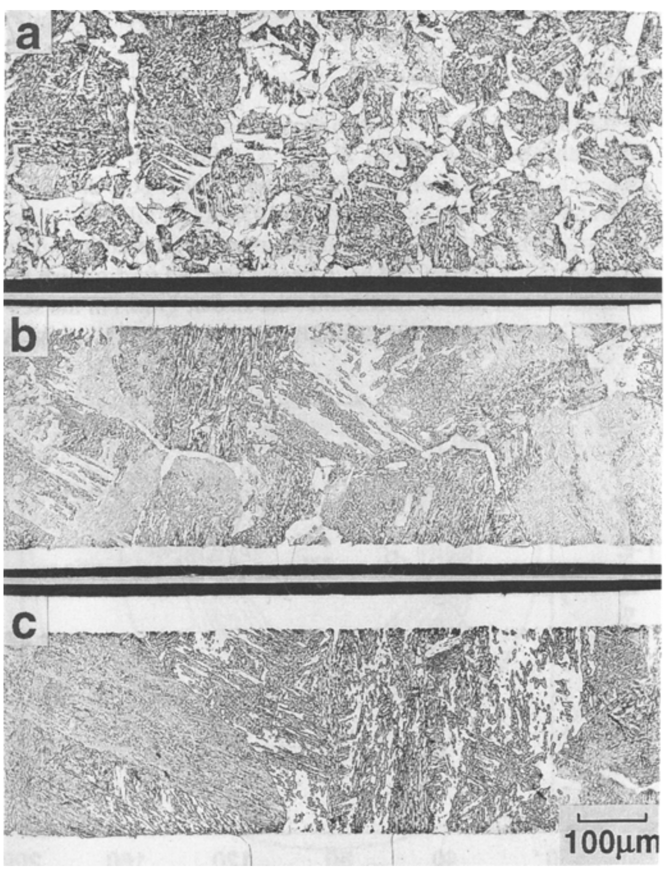

Fig. 1 Optical micrographs of the cross sections of steel B annealed in vacuum at 1000 °C for 10 min (a), 2 h (b), and 9 h (c)

All steels were then subjected to a final annealing as follows. The sheet specimens were first annealed in a vacuum of 10^{-3} Pa at temperatures ranging from 850 to 1100 °C for periods up to 12 h. They were then decarburized in a dry hydrogen gas or a wet hydrogen-argon gas at temperatures from 850 to 1000 °C. Prior to the final annealing, the surfaces of some specimens were roughened or mirror-polished by coarse emery powder or fine alumina powder, respectively, to investigate the effect of surface roughness on texture development. The remaining specimen surfaces were as rolled.

Microstructure, texture, chemical composition, and magnetic properties of the specimens were investigated. Texture was measured by using pole figure and inverse pole figure techniques. These methods were used to measure the pole densities, $(I/I_R)_{hkl}$, where $(I/I_R)_{hkl}$ refers to the ratio of the x-ray integrated intensity of a particular plane for a given sample to the integrated intensity of the same plane for a "random" powder sample. Chemical composition was analyzed by inductively coupled plasma (ICP) or electron probe microanalysis (EPMA). Magnetic properties were measured by a single strip tester with 30 by 100 mm strips or by using ring-shape specimens with inside and outside diameters of 33 and 45 mm, respectively. The strips and rings for the measurement were cut from the specimens and stress relieved by annealing at 800 °C for 1 h in argon atmosphere. To investigate the effects of sheet thickness and stress on magnetic properties, some strip samples were thinned by chemical etching, and magnetic properties were measured by applying tensile stresses up to 9×10^6 Pa in the magnetizing direction.

3. Microstructure and Texture Evolution

3.1 *Manganese Removal Induced Transformation*

Microstructure changes typical of the first annealing stage are shown in Fig. 1. The material depicted (steel B) contains

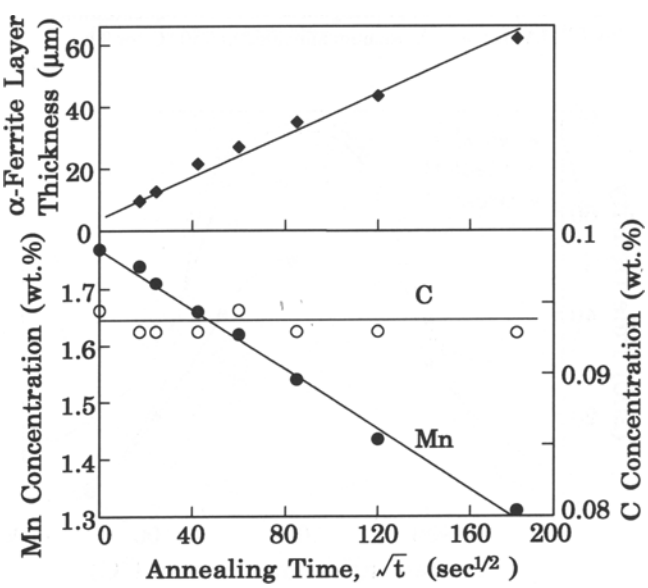

Fig. 2 Variation of thickness of the surface α layer and manganese and carbon concentrations (by ICP) for steel A vacuum annealed at 1000 °C with annealing time

2.8% Si, 2.5% Mn, and 0.1% C before the annealing, and the annealing temperature, 1000 °C, is a γ-phase temperature for steel of this composition. The bainitic structure seen in inner portions of the specimens is a transformation product from γ phase during subsequent cooling. In addition, a bright layer without carbide precipitates is observed to grow slowly from the sheet surface during vacuum annealing. Thickness of the layer becomes about 50 μm after 10 h at this temperature. This surface layer without carbides indicates that an isothermal phase transformation to α occurs near the surface. Similar sluggish transformation to α has also been observed at α/γ duplex phase temperatures; relevant results will be discussed later in Section 3.3. Hereafter, this transformed layer will be called "surface α layer."

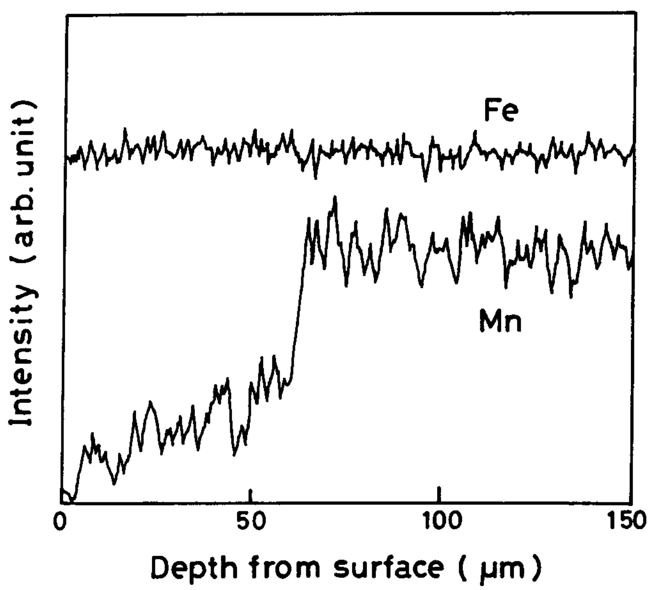

Fig. 3 Depth profiles of manganese and iron concentrations (by EPMA) for steel B vacuum annealed at 950 °C for 9 h

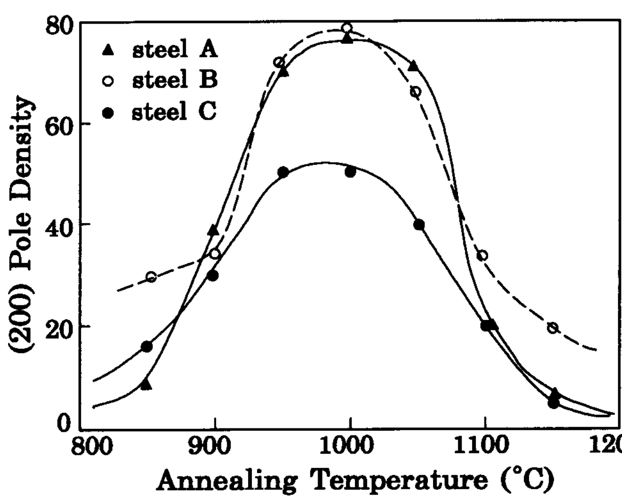

Fig. 4 Annealing temperature dependence of (200) pole density showing the development of (100) texture in the surface α layer. Annealing time, 9 h

As shown in Fig. 2, the thickness of the surface α layer increases with increasing annealing time, t, linearly with the square root of t. Correspondingly, the manganese concentration decreases also linearly with $\sqrt{t}$, whereas the carbon concentration scarcely changes. Note that this compositional analysis is not for the surface α layer but for the entire sheet. The "averaged" manganese concentration decreases by 30% when steel A is annealed at 1000 °C for 9 h. Thereafter, removal of manganese does occur at this stage of annealing, causing formation of the surface α layer.

By the manganese removal, manganese concentration near the surface markedly reduces during vacuum annealing, as shown in Fig. 3. Quantitative analyses by EPMA for steel B annealed at 950 °C for 9 h show that manganese concentrations 10 and 40 μm below the surface (within the surface α layer) are 0.06 and 0.56%, respectively, whereas that of a thickness center portion is 2.6%. It is believed that the significant manganese depletion near the surface increases the chemical potential of carbon and, consequently, that carbon atoms near the surface diffuse into the interior, resulting in a significant reduction in carbon concentration near the surface and thereby causing the transformation to the single α phase (Ref 1). The manganese removal is thought to be due to evaporation of manganese, of which equilibrium vapor pressure is as high as 0.4 Pa at 950 °C (Ref 8). Moreover, the $\sqrt{t}$ dependence of the surface α layer thickness and manganese concentration suggests that the growth of the surface α layer is mainly controlled by diffusion of manganese.

3.2 *Texture Development*

A (100) texture develops in the surface α layer during vacuum annealing. As shown in Fig. 4, (200) pole density increases to more than 50, at the expense of other pole densities, at temperatures ranging from 950 to 1050 °C for all steels under investigation. Under such a proper annealing condition, pole densities other than (200) have been observed to diminish almost to zero. It is noteworthy that the size of grains in the surface α layer having this strongly accumulated texture is as

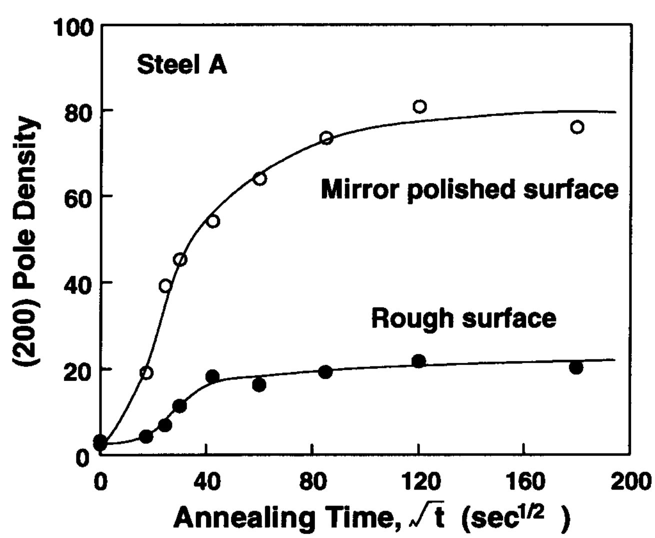

Fig. 5 Effect of surface roughness on the (100) texture development in surface α layer. Annealing temperature, 1000 °C

small as 100 μm when measured in the sheet plane. This texture development is influenced by surface roughness, as clearly seen in Fig. 5. When the sheet surface is roughened with coarse emery powder, the (100) texture development becomes very sluggish, whereas the texture development for mirror-polished surfaces is even faster than for as-rolled surfaces. Moreover, it can be understood from Fig. 5 that the texture development occurs primarily in an early segment of the annealing; in other words, the evolution slows after the thickness of the surface α layer exceeds about 30 μm (see also Fig. 2). These trends imply that the selective driving force for the texture development is surface energy. It is considered that both the $\gamma \rightarrow \alpha$ transformation and the recrystallization of α near the surface are controlled by surface energy so that such a pronounced (100) texture is produced in fine-grained surface layers.

Since the driving force by surface energy determines only the orientation of crystallographic planes parallel to the sheet surface, "in-plane" anisotropy of the (100) texture can vary, depending on processing conditions. Figure 6 illustrates such a variation of the in-plane anisotropy. Textures with some spread

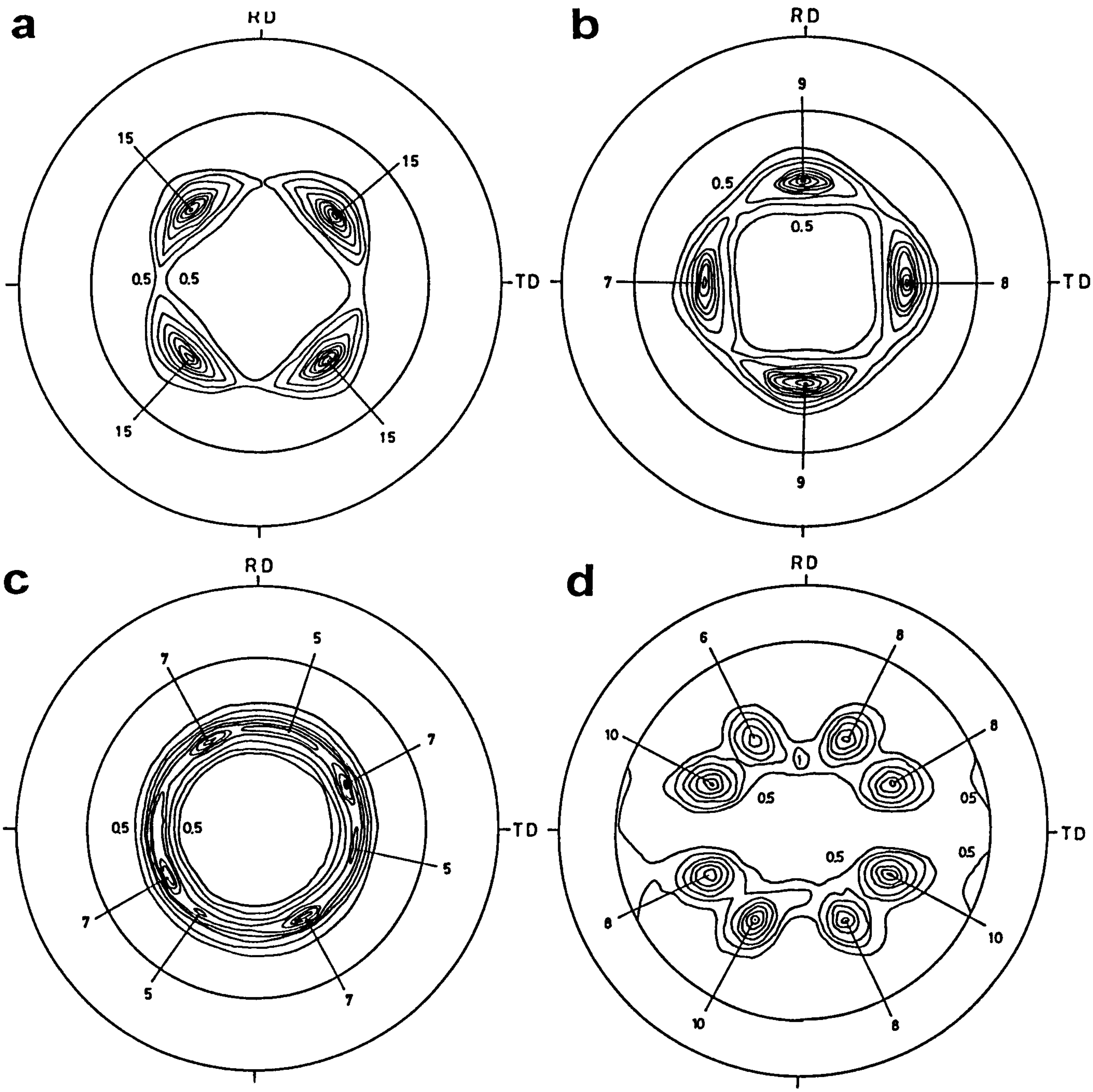

Fig. 6 (110) pole figures showing variation of the in-plane anisotropy of the (100) texture. The textures of steels A (a), C (b), D (c), and E (d) are approximated as (100)[011], (100)[001], (100)[0vw], and (100)[021], respectively. Steels A to D and steel E were vacuum annealed at 950 °C for 9 and 12 h, respectively.

around (100)[001], (100)[011], and (100)[021] and an approximately random cube texture have been observed. Investigation is under way on the mechanism that determines the in-plane anisotropy.

3.3 *Inward Growth of Surface Grains by Decarburization*

At this point of the process, only the surface portion of the sheet possesses (100) texture, and a fairly large amount of carbon, which deteriorates magnetic properties, still remains inside. Subsequent decarburizing annealing at α/γ duplex or γ-phase temperatures causes an inward growth of surface grains as well as a reduction in carbon concentration.

Figure 7 shows cross sections of steel E vacuum annealed at a α/γ duplex phase temperature, 950 °C, for 12 h and the same steel subsequently decarburized at 900 °C (a α/γ duplex-phase temperature) in a wet hydrogen-argon atmosphere. Finer equiaxial grains inside, consisting of dark and bright particles, are due to the α/γ duplex phase at the annealing temperature. Surface α layers also are clearly observed after the vacuum annealing. During the decarburization, the grains in the surface α layer grow into the interior as columnar grains. The columnar grains growing from both surfaces then impinge at the thickness center of the sheet when decarburization is completed. The grain size, measured in the sheet plane, is from 100 to 300 μm when decarburization is completed, and it can increase to about twice the sheet thickness by further annealing. As naturally expected from this microstructure development, the texture of the decarburized sheet is very close to or almost the same as that of the surface α layer formed by the preceding vacuum annealing (compare Fig. 6d and 8). This clearly suggests that, under proper decarburizing conditions, the grains in surface α layers preferentially grow inward, and this grain growth dominates the microstructure change at this stage of annealing.

4. Magnetic Properties

Because of their highly developed (100) texture and fine grain structure, MRD-processed silicon steel sheets exhibit excellent magnetic properties. Typical magnetic properties measured with ring specimens are listed in Table 2. For example, magnetic flux density at 5000 A/m, B_{50}, for the 3% Si steel (steel E) is as high as 1.764 T, and this value increases to more than 1.8 T by reducing the silicon concentration to 2.1% (steel G). On the other hand, the core loss at 1.5 T and 50 Hz, $W_{15/50}$,

Table 2 Magnetic properties measured with ring specimens
Annealed in vacuum at 950 °C for 12 h and subsequently decarburized at 1000 °C (steels E and F) and 950 °C (steel G) in a dry hydrogen atmosphere

Steel	Coercivity, A/m	Relative permeability at 1.5 T	Flux density, T		Core loss, W/kg	
			B_{10}	B_{50}	$W_{10/50}$	$W_{15/50}$
E	7.5	4506	1.601	1.764	0.54	1.37
F	11.3	4407	1.612	1.775	0.64	1.54
G	11.9	4680	1.628	1.805	0.70	1.66

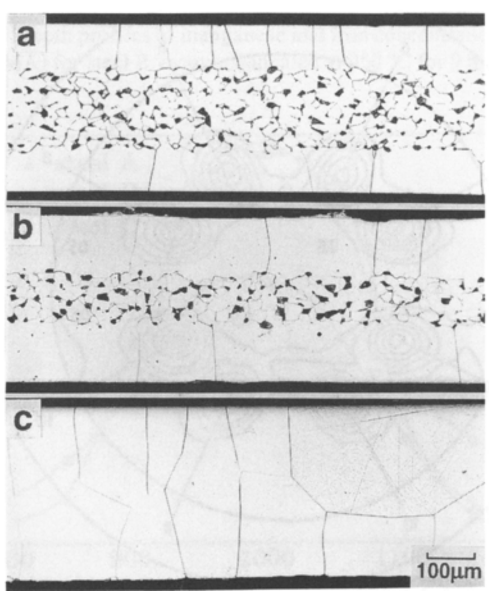

Fig. 7 Optical photographs of cross sections of steel E vacuum annealed at 950 °C for 12 h (a) and subsequently decarburized at 900 °C in a wet hydrogen-argon atmosphere for 30 min (b) and 1 h (c)

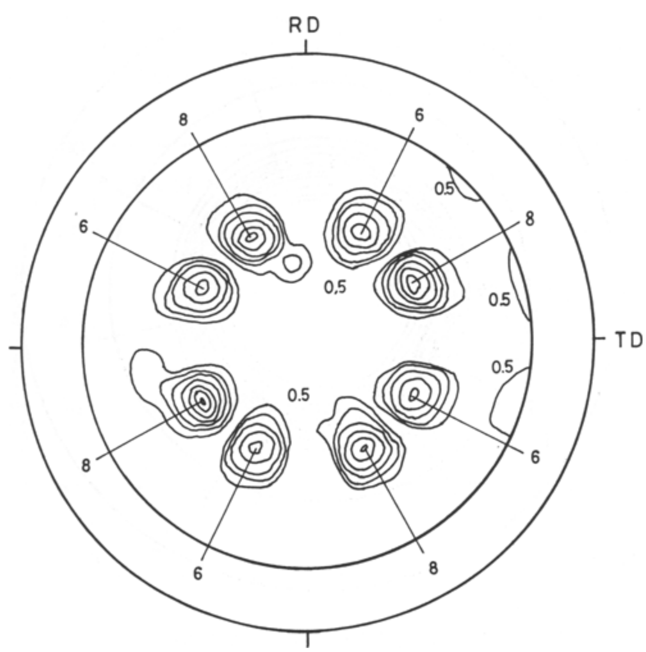

Fig. 8 (110) pole figure for the decarburized specimen shown in Fig. 7(c)

is as small as 1.37 W/kg for the 3% Si steel, and this core loss only slightly increases to 1.66 W/kg when silicon concentration decreases to 2.1%. The relative permeability at 1.5 T is greater than 4400. Thus, since the highest-grade nonoriented silicon steels exhibit, approximately, $W_{15/50}$ of 2.2 W/kg (for 0.5 mm thick sheets) and B_{50} of 1.68 T (Ref 9, 10), the core loss can be reduced by an approximate factor of 30%, and, at the same time, the flux density can be increased by more than 0.08 T by the MRD process.

Small in-plane magnetic anisotropy, which is desired for the magnetic core of rotating machines, is obtained not only by random cube texture but also by (100)[021] texture, as shown in Fig. 9. Since (100)[021] texture consists of two inclined cube components that are rotated by about ±26° from (100)[001] around [100] (see Fig. 6 or 8), the magnetic anisotropies of the two components nearly cancel each other. The change in B_{50} in the sheet plane is about 0.1 T, which is only 6% of the averaged B_{50}, and that in $W_{15/50}$ is 0.4 W/kg for the 3% Si steel.

Another interesting magnetic property is an increased in-plane anisotropy that leads to doubly oriented silicon steels. Therefore, we measured magnetic properties of steel A with (100)[011] texture, which exhibited the largest in-plane anisotropy among specimens made in this experiment. The magnetizing direction is inclined by 45° from the rolling direction in the sheet plane (i.e., easy magnetizing direction). The magnetic flux density at 1000 A/m, B_{10}, for this specimen is about 1.81 T, and the core loss at 1.7 T and 50 Hz, $W_{17/50}$, is plotted as a function of applied tensile stress in Fig. 10. Without tensile stress, $W_{17/50}$ is about 1.4 and 1.0 W/kg for the 0.3 and 0.2 mm thick sheets, respectively, and decreases markedly when tensile stress is applied. Although the decrease in core loss for the 0.3 mm thick sheet does not saturate within the stress of this experiment, the core loss decrement for the 0.2 mm thick sheet saturates beyond the stress of about 6×10^6 Pa. The saturated core loss for the 0.2 mm thick sheet is as small as 0.79 W/kg. This decrease in core loss by the stress is primarily due to a decrement in hysteresis loss. It is also worth noting that although the B_{10} of the specimen is smaller than that of current grain-oriented 3% Si steel sheets (Ref 9), the core loss is comparable or even superior. The mechanism of this reduced core loss, which must relate to the fine grain structure, and modifications of the process to maximize the magnetic anisotropy deserve further investigation.

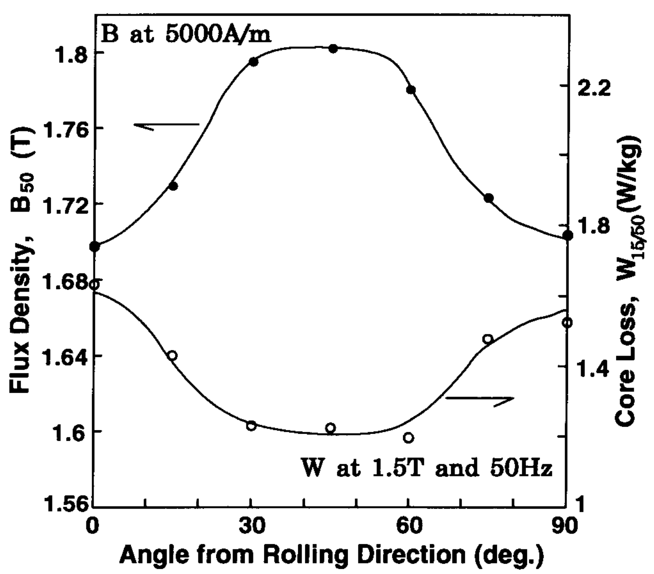

Fig. 9 Magnetic properties measured using strip specimens for steel E vacuum annealed at 950 °C for 12 h and decarburized at 1000 °C in a dry hydrogen atmosphere, showing the in-plane magnetic anisotropy of (100)[021] texture

5. Conclusions

A new manganese removal and decarburization process for developing (100) texture in silicon steel sheets has been described. This two-stage annealing process produces textures with highly accumulated cube planes and a variety of in-plane orientations of cube axes in sheet with the most desired thickness for electrical applications and perhaps with the most suitable grain size structure for the reduction of core loss. Much of the metallurgy surrounding the formation of texture by the MRD process remains unresolved, and modifications may be necessary to commercialize this process. However, since electrical power consumption is quickly rising throughout the world and much of the electricity is dissipated as heat in the magnetic cores of motors and transformers, successful commercialization of the process presents a challenge to both the electrical and the steel industries. The introduction of silicon steel sheets of this kind in commercial apparatus, such as energy-efficient motors for electric vehicles, may be an important factor in obtaining higher system efficiencies through improvement of magnetic steel.

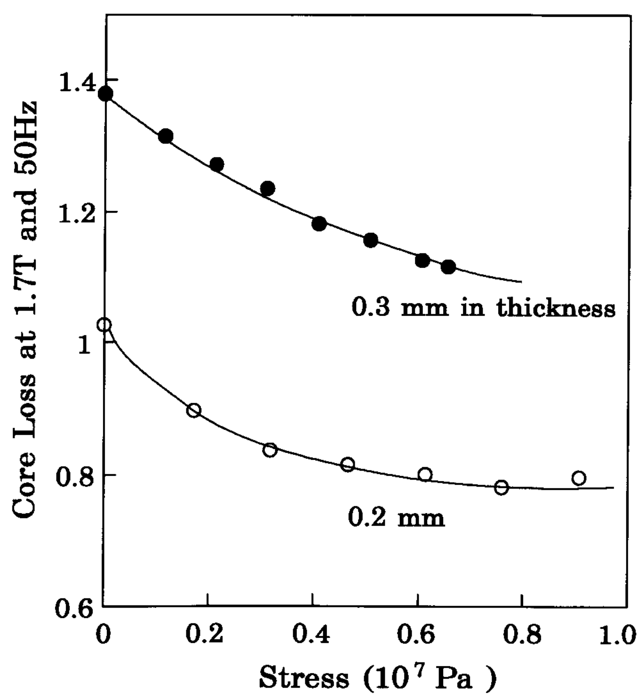

Fig. 10 Core loss in the easy magnetizing direction for steel A with (100)[011] texture. The specimen was vacuum annealed at 950 °C for 9 h and decarburized at 850 °C for 30 min in a wet hydrogen-argon gas atmosphere.

Acknowledgments

The author is grateful to Dr. Y. Maehara, Dr. H. Yashiki, T. Tanaka, and T. Hukagawa for helpful discussion and comments and to S. Uenoya and M. Naga for assisting in experiments.

References

1. T. Tomida and T. Tanaka, *Tetsu-to-Hagané (J. Iron Steel Inst. Jpn.),* Vol 79, 1993, p 1350; *ISIJ Int.*, Vol 35, 1995, p 548
2. K. Detert, *Acta Metall.,* Vol 7, 1959, p 589
3. J.L. Walter, *Acta Metall.,* Vol 7, 1959, p 424
4. R.G. Aspden, J.A. Berger, and H.E. Trout, *Acta Metall.,* Vol 16, 1968, p 1027
5. F. Assmus, K. Detert, and G. Ibe, *Z. Metallk.,* Vol 48, 1957, p 341
6. K. Foster, J.J. Kramer, and G.W. Wiener, *Trans. Met. Soc. AIME,* Vol 227, 1963, p 185
7. V.P. Varlakov and V.M. Romashov, *Fiz. Met. Metalloved.,* Vol 13, 1962, p 671
8. O. Kubaschewski, E.Ll. Evans, and C.B. Alcock, in *Metallurgical Thermochemistry,* 4th ed., Pergamon Press, 1967
9. H. Honma, T. Nozawa, H. Kobayashi, Y. Shimoyama, T. Tachina, and K. Miyoshi, *IEEE Trans.,* MAG-21, 1985, p 1903
10. Y. Shimoyama, K. Miyoshi, M. Tanino, and T. Wada, *IEEE Trans.,* MAG-19, 1983, p 2013